The 2012 World Congress on
Advances in Civil, Environmental, and Materials Research (ACEM' 12)
Seoul, Korea, August 26-30, 2012

Investigation of Flutter Characteristics of Supersonic Experimental Aircraft

Kenichi Saitoh[1)], Masato Tamayama[2)] and Jiro Nakamichi[3)]

Aerospace Research and Development Directorate, JAXA, Tokyo 181-0015, Japan
[1)] ksaitoh@chofu.jaxa.jp, [2)]masato@chofu.jaxa.jp, [3)]jiro@chofu.jaxa.jp

ABSTRACT

The purposes of the present studies are to obtain flutter characteristics of an arrow wing and also to obtain a guide line in applying the linear theory to future SST initial design. The aeroelasticity characteristics were investigated in the transonic regime on the National Experimental Aircraft for Supersonic Transport (NEXST-1) of JAXA. A cranked arrow wing of thickness-to-chord ratio, 3% was adopted as the main lifting surface. In the present studies, the wind tunnel models were designed by FEM and lifting surface theory. The results of not only the flutter tests but also the corresponding flutter analyses are summarized. Based upon the comparisons between the experimental and computational results, discussions are given on the transonic flutter of such a thin wing. The points of concern are; (i) the flutter boundary depends upon the angles of attack, (ii) the model shows so called transonic dip around Mach 1.02, (iii) the flutter is dominated by the bending mode of the outer board, and (iv) the flutter continues in a limit cycle oscillation (LCO). In a result, it is concluded that the flutter speed measured in the wind tunnel tests is 21% lower than the estimated one by the linear theory in case of the isolated gliding flight and 27% lower in case of the launching configuration, respectively. It is emphasized that the methodology to learn the transonic flutter employed in the present studies will be applicable to aeroelastic designs of the future supersonic transport.

NOMENCLATURES

b :	Reference length, half chord length	U :	Velocity or Speed
Cl_α:	Lift coefficient	V_{EAS}:	Equivalent air speed
F, F_3^-, F_z:	Stability Parameters	α :	Angle of attack
f :	Frequency	ρ :	Air density
H :	Height of test section	ρ_{SL}:	Air density at sea level
k :	Reduced frequency	μ :	Mass ratio
M:	Mach number	ζ :	Damping ratio
m_g:	Generalized mass	η :	Loss Factor
P_0:	Total pressure	$(\ )_\infty$:	Quantity related to uniform flow

1. INTRODUCTION

In 1963, a supersonic transport(SST) development program was initiated in the U.S. At the early stage of the conceptual design of Supersonic Commercial Air Transport (SCAT), several kinds of concepts were offered by Lockheed Martin and Boeing companies. Variable swept-back wing types and conventional wing types were included in the proposals to permit high performance operations at various speeds. After modifications and refinements of the airframe were introduced, both concepts from the Boeing and Lockheed Martin were merged into B-2707-300, which became a baseline of SST considered later on.

Unfortunately, in 1971, the SST Program was ceased by the US Governments. The flutter problem which comes from so called transonic dip had not yet been resolved at that time. Since an arrow wing tended to become larger and more flexible, aeroelasticity was a major consideration in the preliminary design for which FEM structural analysis and sophisticated aerodynamic loading analysis were required.

In the course of the studies in the U.S. SST Program, remarkable progresses were made in the field of aeroelasticity design technology; for example, the ATLAS reached the level that it could estimate the SST flutter speed with high accuracy in the trade-off among flutter speed, structural weight and aerodynamic drag.

Douglas and Boeing have continued HSCT(High Speed Civil Transport) Program under the contract with NASA since 1986. NASA has also proceeded their own program, HSR(High Speed Research) since 1990.

In Japan, National Experimental Aircraft for Supersonic Transport (NEXST-1) project was started at JAXA in the beginning of 1990's. The principal objectives of the project were to assess a natural laminar wing to reduce the aerodynamic drag and to validate the computational method to design the wing for an advanced supersonic vehicle. The experimental aircraft was a 11% scaled model which represents a 100-seater cruising at Mach 2.0.

The present studies are to investigate the correlations between flutter test result and linear theory which will be utilized to design an arrow wing for the experimental aircraft.

2. AEROELASTICITY DESIGN OF THE EXPERIMENTAL AIRCRAFT

2.1. Outline of the Flight Test

The aerodynamic geometry of the vehicle was produced by the use of CFD optimization technique. The upper and lower surfaces of the main wing were designed so that the laminar flows would spread as wide area as possible. The purpose of the flight test was to confirm that the pressure distributions on the main wing surfaces at cruise condition of Mach 2.0 are as intended to be at the design stage.

The vehicle was planned to be boosted by a rocket motor for the launch. It was to be separated at the altitude about 20km at Mach 2.5. After separation, it would start gliding flight and offer two chances to measure the pressure distributions on the lifting surfaces at Mach 2.0; one is at higher altitude with low *Re* number, the other is at lower altitude with high *Re* number, keeping the angle of attack constant.

Finishing the data acquisitions, the vehicle was intended to be decelerated and to be recovered hopefully without any structural damages using the parachutes and airbags.

it was needed to confirm the aeroelastic safety in both phases of isolated gliding and launching configuration s flight. The photos of the models mounted in the wind tunnel are shown in Fig.1 and Fig.2. The configurations for the isolated flight and for the launching are drawn in Fig.3 and Fig.4.

Fig.1 Isolated Flight Configuration (Wind Tunnel Model)

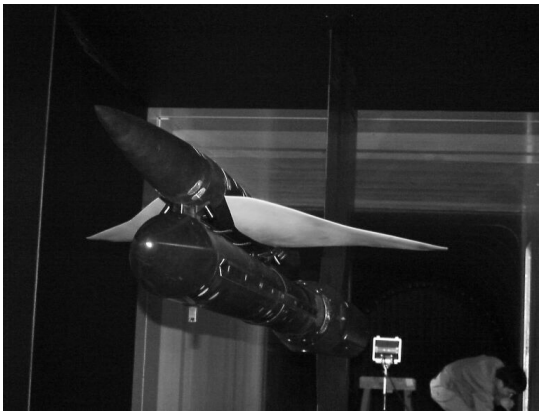

Fig.2 Launching Configuration (Wind Tunnel Model)

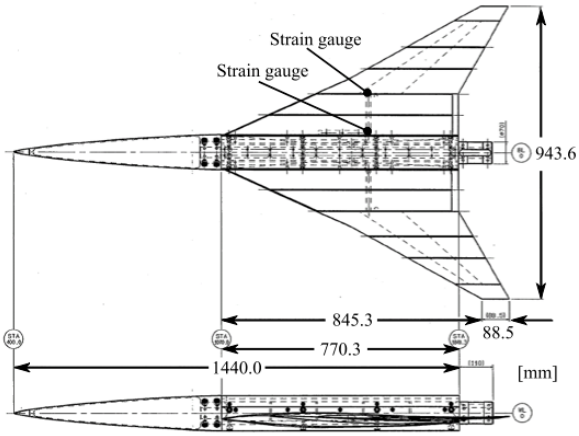

Fig.3 Isolated Flight Configuration

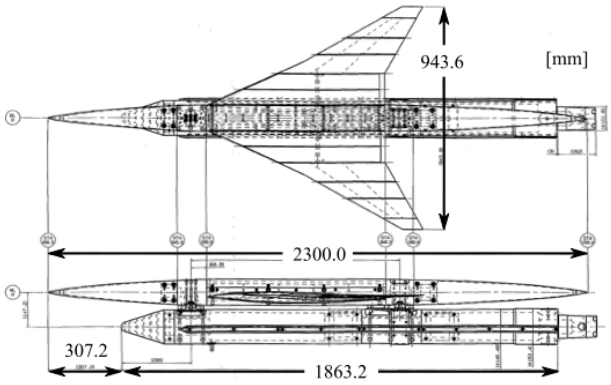

Fig.4 Launching Configuration

2.2. *Outline of the Vehicle*

The main surface of the vehicle is a cranked arrow type with kinked trailing edges at about 40% semi-span position. The thickness-to-chord ratios are 3.7% at inner sections(between the fuselage and the kink) and 3.0% at outer sections(between the kink and the wing tip). As for the structural configuration, the outer board is made of solid aluminum alloys of 2124-T851 or 2024-T62, while the inner board consisted of a spar-ribs structure. The tail surfaces are also made of solid alumina alloys. The fuselage is a multi-monocoque structure which has spaces enough to load the measurement equipments, the parachutes, air bags and so on.

2.3. *Criteria for Aeroelasticity Design for Experimental Aircraft*

In 1992, the Federal Aviation Administration (FAA) Regulations, Part 25 were revised about the requirements to be imposed on flutter, since remarkable progresses had been made in the developments of integrated design tools and applications methodology for flutter. So it was concluded that the flutter margin for Transport Category should be no less than 15% of design diving speed with respect to the equivalent air speed for constant altitude case as well as constant Mach number case.

Supersonic Transport may experience a cruel situation of flutter due to transonic dip, which must be investigated carefully in the structural design stage.

Many studies have been conducted about the flutter of arrow wings so far. Similar wings were investigated by so many researchers. For examples. Doggett Jr., R. V.,Durham, M. H. ,Keller,D. F. and other people have revealed the influences of engine nacelles, upper surface fins as well as span length on arrow wing flutters. According to those studies, the amount of decrease in flutter speed at Mach 0.98, that is, at the bottom of the transonic dip, seems to be about 20% of estimated values by the linear theory.

In the present case, it was also assumed that the flutter speed decreases by 20% from the estimation by linear theory at the bottom of the transonic dip, Mach 0.98, as was suggested in the above researches. Moreover, a safety factor of 1.25 was applied to the flutter margin to account for uncertainties. The total flutter margin is set to be 50% in comparison between the design flutter speed and the flutter speed computed by linear theory assuming the structural damping to be 0.01.

The flutters of ailerons and rocket fins are also of importance and must be care of. Those flutters were also investigated in the wind tunnel tests, respectively, though they are not described in the present paper.

3. WIND TUNNEL MODEL

3.1. Aeroelasticity Similarity

The flutter characteristics of main surface were checked not only for the isolated flight configuration but also for the launching configuration. The aerodynamic similarity between the experimental aircraft and the wind tunnel model is summarized in Table 1.

The scale of the model was determined to be 1/5 from the viewpoint of the blockage ratio for the wind tunnel test section. The design point to look at the flutter is at Mach 0.9 and at altitude, 6,000 fts, which corresponds to the wind tunnel total pressure,80kPa.

	Experimaental Aircraft	Model
Mach	0.9	0.9
V_{TAS} $[m/s]$	299.9	284.1
ρ $[kg/m^3]$	1.023	0.664
h $[m]$	1,829	
P_0 $[kPa]$		80
q[kPa]	46.01	26.80
ρ_{0SL}	1.225	1.225
V_{EAS} [m/s]	274.1	209.2
scale	1.00	0.200
Velocity	1.00	0.947
Density	1.00	0.649
Frequency	1.00	4.74
Mass Ratio	1.00	0.0052

Table 1 Similarity Law

The 2mx2m Transonic Wind Tunnel (TWT) at Chofu Aerospace Research Center/JAXA was used for the tests. It is needed that the flutter must occur in the operation range of the wind tunnel to capture the hard flutter points for the validation of analytical tools. If the model is designed faithfully in consistent with the similarity relations shown in table 1, the flutter point can not be captured in the flutter tests. Therefore the stiffness of the model was reduced by 0.38 so that the flutter might occur in the operation range.
In this case, the mass ratio in the wind tunnel test becomes too large to keep the similarity to the actual flight.

3.2. Geometries and the Structural Configurations of the Wind Tunnel Model

The wing model structures consist of the spar-ribs (Al7050) and skins. The spar-ribs were designed to simulate the wing vibration modes and frequency distributions of the experimental aircraft. Urethane forms were utilized for the skins to retain the aerodynamic shapes and to give little disturbances to the appropriate stiffness distributions designed so as to simulate the vibration characteristics of the experimental aircraft.

The fuselage of the aircraft and the rocket motor for the launching configuration were assumed to be rigid. Rear and fore fuselage were made of a certain resin and the middle part was a circular cylinder of steel, SS400. The control surfaces, such as ailerons, vertical fin, horizontal stabilizers and rocket fins were not considered. Strain gauges were embedded on the main spars of the wing model to monitor the strains caused by wing bending and torsion motions, respectively.

Two kinds of wings, nominal stiffness model and stiffer model, were prepared to avoid a failure in capturing the flutter point in the wind tunnel operation range due to the errors of the linear theory and other uncertainties. To show the stiffness levels of the two models, the lowest frequencies are compared with each other together with that of the experimental aircraft in Table 2.

	Frequency[Hz]	Reduced Frequency (DesignPoint)
Nominal Wing	21.0	0.18
Stiffer Wing	24.8	0.21
Experimental Aircraft	11.7	0.47

Table 2 Frequencies of First Bending Mode

3.3. Fundamental Vibration Modes

The results of the structural vibration analysis by NASTRAN are shown in Figs.5. The right side is for nominal wing and the left side is for the stiffer wing.
The mode displacements are normalized by the maximum value in each figure. The bold solid lines show the nodal lines and the fine solid lines represent the contours of displacements in every 0.2 increment. In Figs. 5, the first 4 figures show the bending modes of the nominal and stiffer wings. The next 2 figures are the first torsion modes.

.

Three kinds of GVT were conducted; the first one was done outside of wind tunnel for the nominal stiffness full span model(case1); the second was done also outside of wind tunnel for the stiffer model(case2); the third one was done in the wind tunnel for asymmetric configuration which has a nominal stiffness wing on the right side and a stiffer wing on the left side(case3). This asymmetry full span model was tested which was supported by sting-strut system through a roll-free supporting system, though the roll freedom was kept locked.

Mode			GVT			Analysis
			In Wind Tunnel	Outside Wind Tunnel		Frequency[Hz]
#	Left Wing	Right Wing	Frequency [Hz]	Frequency [Hz]	Structural Damping g	
1		○	19.6	21.0	0.012	20.1
2	○		25.1	26.5		26.9
3		○	60.6	58.6	0.013	57.1
4	○		70.2	66.4		71.4
5		○	114.1	107.8	0.018	106.4
6	○		132.9			129.1
7		○	144.7			144.2
9	○		183.4			183.0

Table 3 Comparisons of Frequencies Between GVT and Analysis

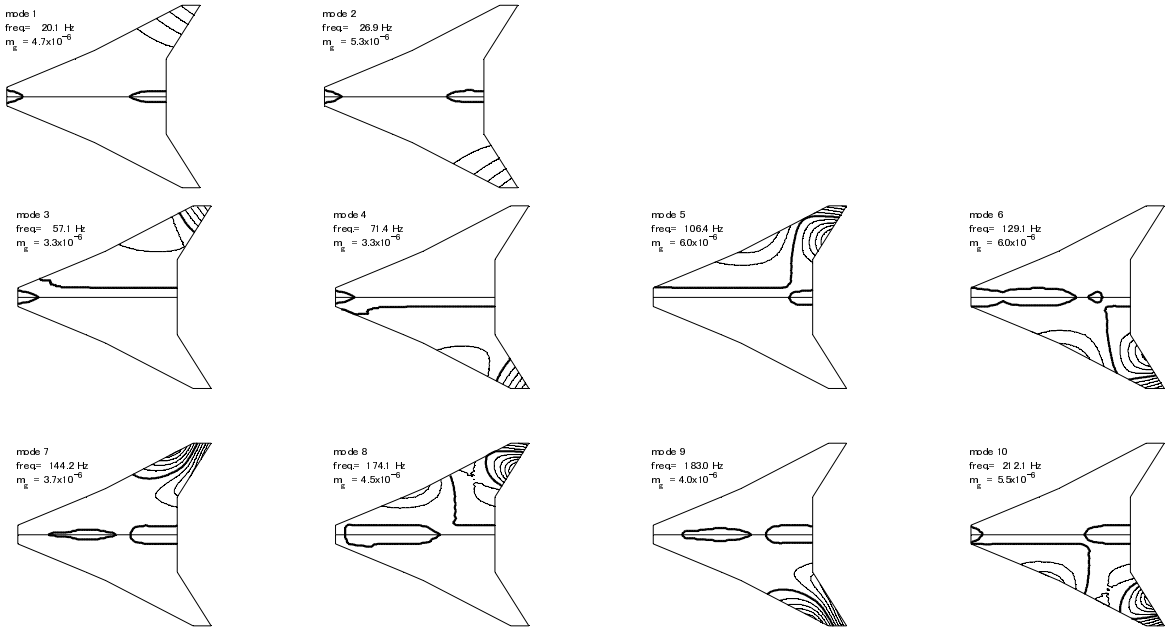

Fig.5 Fundamental vibration modes of isolated flight configuration
-Computed result- (m_g : generalized mass)

In case3, the model was being mounted on the sting-strut system as was done in the flutter tests. In Table 3, the GVT results (case1~3) and the analytical results are shown together with the measured structural damping coefficients in GVT(case1).

4. FLUTTER ANALYSIS

4.1 Linear Theory

Flutter analysis were conducted by the use of an almost single software for the solutions of vibration modes, unsteady air forces and flutter equations, in which FEM, Doublet Point Method(DPM) and *P-k* method were employed.(Fig.6).

According to the FAA regulations, the flutter margins should be confirmed for both of constant altitude case and constant Mach number case.

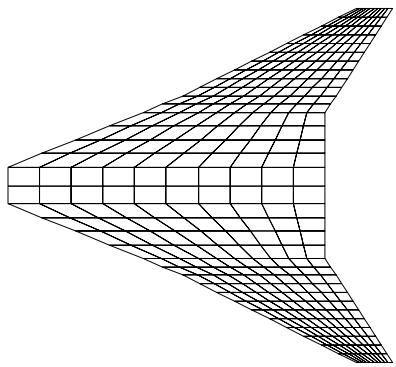

Fig.6 Panel division for DPM

In Fig.7, the V_{EAS}'s (Equivalent Air Speeds) are plotted on mass ratio vs. Mach number plane with parameters of total pressures and air densities. The solid line mesh indicates the computed stability boundary. The dotted line mesh shows the air speeds realized in the wind

tunnel for each combination of Mach number and mass ratio. The intersection of the stability boundary and the air speeds plane shown by a bold solid line in Fig.7 is the flutter speeds which are expected to be actually observed in the wind tunnel. The identical bold line is projected in a Mach number vs. V_{EAS} plane in Fig.8. It is found that flutter will occur at mass ratios between μ =241.7~72.6(ρ = 0.3~1.0 ρ_{SL}).

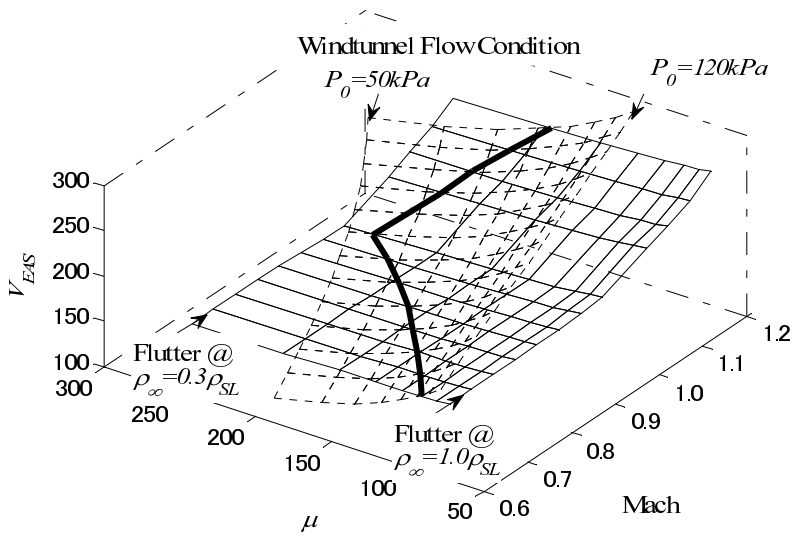

Fig.7 Wind tunnel operation range (Dotted mesh)
Flutter speeds on Mach- μ plane (Solid mesh) -computed-

It is noted here that the flutter boundary indicated (bold line) in Fg.7 and 8 can keep a consistent relations between the actual wind tunnel flows and the computational conditions, especially with respect to the mass ratios which have a significant influence on flutter.

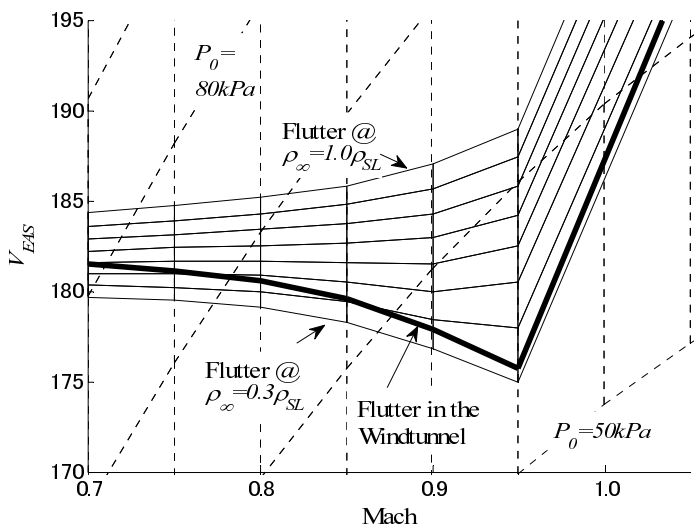

Fig.8 Flutter Boundary in Mach vs. V_{EAS} Plane

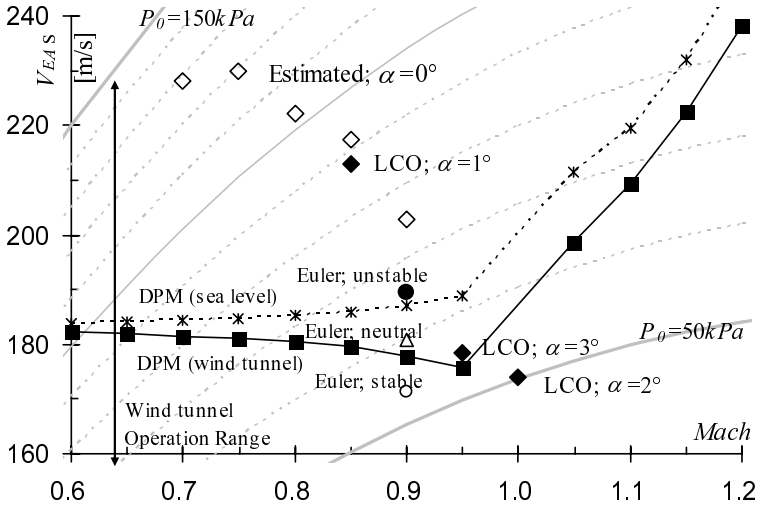

Fig.9 Flutter boundaries

4.2. Euler Analysis

Flutter simulations were conducted for the cases of Mach 0.9 (V_{EAS}=171*m/s*, 181*m/s* and 190*m/s*) with the structural damping, 0.022, using CFD Euler code. At V_{EAS}=171*m/s*, all vibration modes are converging, while at V_{EAS}=190*m/s*, some modes are diverging. All modes are in sinusoidal oscillations during the flutter at V_{EAS}=181*m/s*. Therefore, the flutter velocity (181*m/s*) estimated by Euler simulation is consistent with the computed flutter speed(178*m/s*) by the linear theory assuming the structural damping, 0.01.

5. WIND TUNNEL TESTS

5.1. Outline

Flutter tests were conducted in the circular flow type 2mx2m TWT. Four test sections are provided as No.1~No.4. For the present studies, No.1 and No.3 carts were used. The isolated flight configuration model was tested in the No.1 cart and the launching configuration model was done in the No.3 cart. The No.1 cart is walled by porous plates of which open ratio is 20%. The No.3 cart is walled by slit plates over the ceiling and floor of which open ratio is 6%. In both cases, sting-strut supporting systems are available and were adopted for the flutter tests.

The flow conditions for the tests are specified by Mach number and the total pressure with control of the total temperature of the flow. The signals from the strain gauges embedded on the spars of wing model are taken out of the wind tunnel in order to monitor the wing responses. Wind turbulence was made use of to give the model excitation because unfortunately the drive apparatus is not equipped in the facility.

5.2. A Method to Avoid Destruction of Flutter Model

The model is supported through the roll-free supporting system as mentioned before. It was found in the GVT that, when the roll-freedom was locked, the vibration characteristics of the right and left wings could be obtained independently. On the other hand, when the roll motion was released, the lowest frequencies became higher than those of roll-locked case.

It had been pre-estimated by the linear analysis that symmetry flutter would be critical in both isolated flight and launching configurations. The symmetry flutter would occur in either roll-free or roll-locked case. Therefore the symmetry mode flutter, if occurs, does not cease.

For the isolated flight configuration, the asymmetry full span model(right wing is nominal one; the other is stiffer) was tested with the roll-freedom locked. If the flutter occurs, the roll-freedom is released. Then, the flutter will cease because the frequencies of the first bending modes will increase comparing with the roll-locked case.

As an alternative way to protect the model from destruction, it is effective to quickly change the angle of attack, while it is needed that the dependency of flutter speed on the angle of attack has been revealed. Beside above, in case, safety nets was utilized in order to protect the rotor blades of TWT from the pieces of the broken model.

5.3. Results of Tests

Some discussions are given on the results of the flutter tests for the isolated flight configuration. The wing responses were monitored in wide ranges of Mach numbers from 0.7 to 1.05 , total pressures from 50kPa to 109kPa and the angles of attack, 0° , 1° , 2° and 3° . In order to determine the flutter point, subcritical prediction methods proposed by Zimmerman et al.(1964), Matsuzaki et al.(1981) and Torii et al.(1999) were applied respectively to the present cases. Some hard flutter points were also obtained.

In Zimmerman's method, the frequencies and damping ratios, ζ of the two vibration modes(first bending and first torsion mode) dominant in flutter are needed. They were obtained by Random Deck Method (RDM) . The obtained frequencies and loss factors, $\acute{\eta}$ (defined by $\acute{\eta}=2\zeta$) are indicated by solid and empty circles with respect to V_{EAS} in Figs.10(a),(b)~12,(a),(b) at Mach, 0.7,0.8 and 0.9,respectively. The corresponding values computed by DPM are also shown in the same figures by solid and dotted lines. The measured loss factors steeply go down in the case of Mach, 0.8, which is similar trend to the computed results(Fig.11(b)). DPM predicts flutter around V_{EAS}=180*m/s* at Mach 0.7~0.9. The actual flutter speeds, however, seem to be much higher than that as is seen in Figs.10(b)~12(b). Usually, it is quite difficult to estimate the flutter points by the behaviors of loss factors.

On the other hand, stability parameters, F suggested by Zimmermann, F_3^- by Matsuzaki and F_z by Torii are plotted using ▲, □and ○, respectively, in Fig.10(c)-12(c). The flutter speeds estimated by the three methods were averaged and plotted by ◇ in Fig.9 and summarized in Table 4.

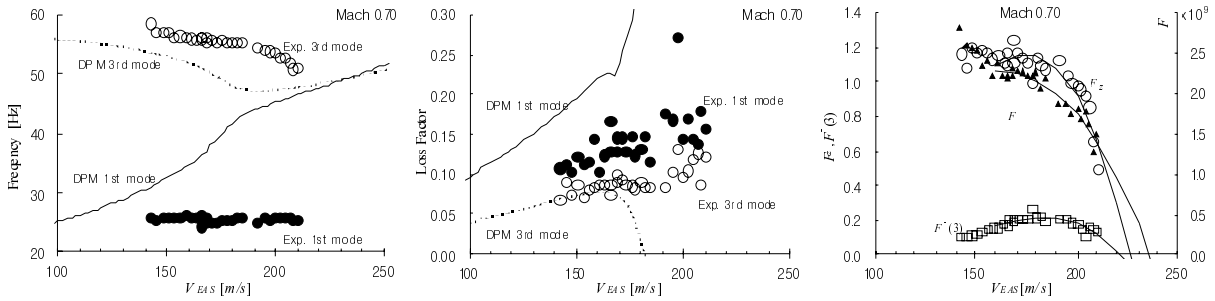

(a) Frequencies (b) Damping (c) Subcritical stability parameters

Fig.10 Vibration characteristics with respect to V_{EAS} (M=0.7, α =0°)

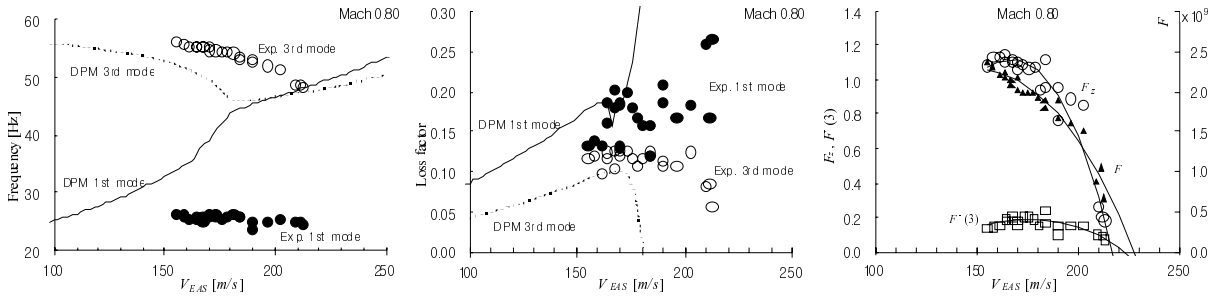

(a) Frequencies (b) Damping (c) Subcritical stability parameters

Fig.11 Vibration characteristics with respect to V_{EAS} (M=0.8, α =0°)

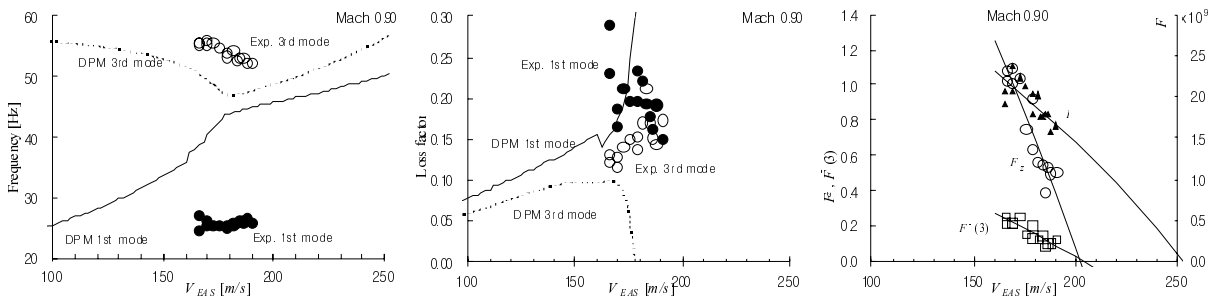

(a) Frequencies (b) Damping (c) Subcritical stability parameters

Fig.12 Vibration characteristics with respect to V_{EAS} (M=0.9, α =0°)

Mach	V_{EAS} [m/s]	α [deg.]	f [Hz]	remark
0.7	228	0.0	-	subcritical
0.8	222	0.0	-	subcritical
0.85	213	1.0	45.2	hard point
0.90	203	0.0	-	subcritical
0.95	178	3.0	39.8	hard point
1.00	174	2.0	36.9	hard point

Table 4 Flutter Points and Related States

In the course of present studies, hard flutter points were caught at Mach 0.95 with angle of attack, 3° , at Mach 1.0 with angle of attack, 2° and at Mach 0.85 with angle of attack,1° , though subcritical methods had been intended to be used. The data are also included in table 4 and indicated by ♦ in Fig.9. All of the actually observed flutters were Limit Cycle Oscillations(LCO), in which the outer board mode is dominant. The dependencies of LCO on the angles of attack were confirmed from the fact that flutter did cease even if the angle of attack reduced only by a small amount.

There is so called transonic dip around Mach 1.02 in the case of angle of attack, 0° (Fig.9). Comparing the flutter speeds, V_{EAS}=222*m/s* (Mach 0.80 ,angle of attack 2.0°) with V_{EAS}=174*m/s* (Mach 1.0, angle of attack 0°), it is found that flutter speed drops by 21%, as is expected at the earlier stage.

Incidentally, in the case of the launching configuration, flutter occurred at V_{EAS}=182*m/s* at Mach, 0.95 with angle of attack 2° . It is 27% drop comparing with the result of the linear flutter analysis.

6. CONSIDERATIONS ON EXPERIMENTAL RESULTS

In the transonic regime, it is well known that the flutter speed is much lower than that estimated by linear theory. However, the flutter boundary found in the present experiments is much higher than that computed by linear theory.
The considerations on the contradiction will be given in the following sections.

6.1. Structural Factors

Effects of Change of Fundamental Frequencies

The flutter model tested in the present studies consists of spar-ribs of aluminum to provide the stiffness and urethane forms to maintain the aerodynamic geometry. The stiffness of the model can change because of separations of the bonding and the plastic deformation of the spar during the vibration and flutter tests.
Though, in the present cases, big changes of the frequencies were not observed, the peaks of power spectrum of some modes sometimes moved. These mean values and standard deviations, σ are shown in table 5.

mode	Nominal Freq [Hz]	σ [Hz]	σ [%]
1	19.6	0.15	0.8
2	25.1	0.14	0.6
3	60.6	0.99	1.6
4	70.2	1.28	1.8
5	114.1	4.91	4.3
6	132.9	1.29	1.0
7	144.7	2.61	1.8
8	183.4	3.22	1.8

Table 5 Variations of Frequencies during Tests

mode		magnitude of eigen vector	ratio [%]
1	0.8575	1.0000	55.3
2	0.0961	0.1120	6.2
3	0.5021	0.5855	32.4
4	0.0278	0.0324	1.8
5	0.0108	0.0126	0.7
6	0.0018	0.0021	0.1
7	0.0493	0.0575	3.2
8	0.0021	0.0024	0.1
9	0.0022	0.0025	0.1
10	0.0001	0.0002	0.0

Table 6 Contributions of Fundamental Vibration Modes to Flutter (M=0.8)

In the flutter analysis, the flutter mode is assumed and approximated by superposing a number of the fundamental vibration modes. In order to investigate the effects of these approximation errors on the flutter analysis, the flutter speeds(V_{EAS}) and frequencies, obtained using the lowest N modes (N=1,2,3,….10) are compared based upon the case of N=10 in case of Mach, 0.8. The comparisons are shown in Fig.13. If more than seven modes are used, the accuracy can be maintained enough. In case of seven modes or less, however, 6 or 7 % errors are possible at most in flutter speeds.

Table 6. shows the contribution of the individual mode to the flutter in case of Mach, 0.8. The lengths of the eigen-vectors corresponding to the eigen-value which gives the flutter speed and frequency are compared. The 10 modes analysis gives the flutter speed, V_{EAS}.=180*m/s*. Each vector length is normalized by that of the first bending mode(most dominant one). The mode 1 and 3 are dominant. The modes 2,4,and 7 are subdominant. The mode 7 (torsion mode of the outer board) is of importance and will have influences on the computed results.

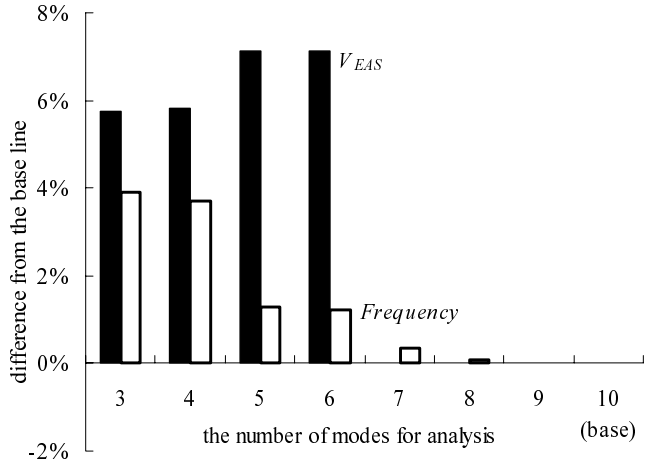

Fig.13 Effects of approximation orders
on flutter speeds (M=0.80) - computed -

Fig.13 shows the sensitivities of the computed flutter speed with respect to the errors of the fundamental frequencies. In this example, even if the mode 1 or mode 7 has 5% error, the resulted error in the flutter speed is within 1%. However, if the mode 3 has 5 % error, then the error is more than 5% in the flutter speed.

Effects of Elastic Mode of Supporting System

In the present experiments, The models are supported by the sting-strut system through the roll free supporting apparatus. The vibration modes of the those structures might have influences on the flutter. In a flutter analysis taking into account of the sting vibration mode, , for example, it resulted in 3.1% increase in the flutter speed

6.2. Aerodynamic Factors

It is known that the unsteady aerodynamic forces computed by potential theory are over estimations. It leads that computed flutter speed is conservative and lower than the calculated one. Saitoh et al.(2010) examined the wall effects about 2D flutter model of which span-to-chord ratio H/2b is 2.4. In that case obtained flutter speed in the wind tunnel test was 20% larger than that based on the linear theory. It seems to come from wall effects. Other uncertainties are possible in the wind tunnel tests, for example, blockage ratio, measurement accuracy of total temperature to control the flows, flow turbulences and so on. Incidentally, the span-to-chord ratio, H/2b of the present 3D model is 2.6 for the root section and 23 for the tip section.

6.3. Validity of the Aeroelastic Design

There are uncertainties in the wind tunnel tests as are mentioned above. The 21% difference, however, can not be explained by the present efforts. Nonlinear analysis should be done for the design of the wind tunnel models, that means, for the design of future SST to check the transonic flutter problems.

CONCLUSION

A series of flutter tests were conducted in the course of the structural design of the National Experimental Aircraft for Supersonic Transport (NEXST-1) of JAXA., aiming to accumulate more data of the arrow wing flutter in transonic regime, for the design of future SST. The outlines of the flutter tests and related methodologies have been described. Some comments are given based upon the present studies.

Correlations between flutter test result and linear theory which will be utilized to design cranked arrow wings of the future SST have been investigated. The points of concern in the present flutter test results are;

1) The model shows so called transonic dip around Mach 1.02. if they are compared with the linear analysis, the drop of the flutter speeds are 21% for the isolated configuration and 27% for the launching configuration, respectively. The flutter boundary depends upon the angles of attack. The flutter is dominated by the bending mode of the outer board and the wing continues in a limit cycle oscillation (LCO).

2) Based upon the present studies as well as the past researches done in the past, a criteria has been proposed for the aeroelastic design; a 50% flutter margin is appropriate when linear theory is employed to estimate the stability boundaries, even considering the transonic dip.

3) It is extremely difficult to keep the similarity laws between the wind tunnel tests and actual flight. It is important to confirm the correlations between the test results and the computed ones with respect to mass ratio. It is noted here that the points on the flutter boundary indicated (bold line) in Fg.7 and 8 keep consistent relations between the wind tunnel flows and the computational conditions with respect to the mass ratios which have a significant influence on flutter.

4) An effective way was proposed to protect the flutter model from destruction. It is effective to control the roll freedom in the present case.

5) In flutter tests, it is quite difficult to predict flutter speed by loss factors(damping coefficients). On the other hand, the subcritical methods are valid as were applied in the present studies.

6) There are uncertainty factors in the wind tunnel tests as were considered in the present studies. The 21% difference, however, can not be explained by the present considerations.

It is emphasized that the methodology to learn the transonic flutter employed in the present studies will be applicable to the aeroelastic designs of the future supersonic

transport, though it is quite difficult to maintain the aeroelasticity similarity between the wind tunnel tests and the actual flight conditions.

REFERENCES

McLean, F. E. (1985), " Supersonic Cruise Technology," NASA SP-472.
Turner, M. J. and Grande, D. L. (1977), " Study of Metallic Structural Design Concepts for an Arrow Wing Supersonic Cruise Configuration, " NASA CR-2743.
Hitch, H. P. Y. (1972), "Concorde Dynamics – a Review," AIAA 72-381.
Ruhlin,C. L. and Pratt-Barlow,C. R. (1981), " Transonic Flutter Study of a Wind-Tunnel Model of an Arrow-Wing Supersonic Transport," AIAA 81-0654.
Doggett Jr., R. V. and Ricketts,R. H.(1977), " Some Experimental and Theoretical Flutter Characteristics of an Arrow-Wing Configuration," AIAA 77-422.
Doggett Jr., R. V. and Ricketts, R. H.(1980), " Effects of Angle of Attack and Ventral Fin on Transonic Flutter Characteeristics of an Arrow-Wing Configuration," NASA TM-81914.
Durham, M. H., Cole S. R., Cazier Jr., F. W., Keller,D. F., Parker,E. C. and Wilkie,W. K. (1990), " Experimental Transonic Flutter Characteristics of Supersonic Cruise Configurations," AIAA 90-0979.
Keller,D. F. and Bullock,E. P. (1991) , " Span Reduction Effects on Flutter Characteristics of Arrow-Wing Supersonic Transport Configurations," NASA TP-3077.
Schuster,D. M., Spain,C. V., Turnock D. L., Rausch,R. D., Hamouda,M., Vogler,W. A. and Stickwell,A. E.(1999), " Development, Analysis and Testing of the High Speed Research Flexible Semispan Model," NASA CR-1999-209556.
Silva,W. A., Keller,D. F., Florance,J. R., Cole,S. R. and Scott,E. C. (2000), " Experimental Steady and Unsteady Aerodynamic and Flutter Results for HSCT Semispan Models," AIAA 2000-1697.
Suzuki,K., Hosoe,N.,Nakamura,M.,Kike,A.,Iijima,Y.,Oguni,Y.,Kawamoto,I. and Ebihara,M. (1995) , "Refurbishment of the NAL 2mx2m Transonic Wind Tunnel Test Section", NAL TM-674. (written in Japanese)
Zimmerman,N. H. and Weissenburger,J. T.(1964), " Prediction of Flutter Onset Speed Based on Flight Testing at Subcritical Speeds," J. Aircraft, 1, pp.190-202
Matsuzaki ,Y. and Ando,Y. (1981), " Estimation of Flutter Boundary from Random Responses Due to Turbulence at Subcritical Speeds," J. Aircraft, 18, pp.862-868
Torii, H. and Matsuzaki,Y. (1999), "New Flutter Prediction Method Based on ARMA Model (Part 1) Proposal of New Flutter Prediction Parameter", J.JSASS,47, pp.443-448 (written in Japanese)
Cole Jr.,H. A. (1973), " On-line Failure Detection and Damping Measurement of Aerospace Structures by Random Decrement Signatures," NASA CR-2205.
Abel, I ., Perry, B. III and Newsom,J. R.(1982), " Comparison of Analytical and Wind-Tunnel Results for Flutter and Gust Response of a Transport Wing With Active Controls," NASA TP-2010.
Saitoh,K., Tamayama,M. and Yoshimoto, Y. (2010), "Unsteady Aerodynamic Loads on Occurrence of Flutter ", Proceedings of the 48th Aircraft Symposium, pp.136-140 (written in Japanese)